

2018 NM WRRI Student Grant Final Report

Student Researcher: Kyle Stark; kyle.stark@student.nmt.edu

Faculty Advisor: Dr. Daniel Cadol; daniel.cadol@nmt.edu

Budget update:

Budget Item	Description	Cost
Salary	Summer student assistance during monsoon season (July-September).	\$1,344
Fringe Benefits	2% for NMT fringe benefits	\$266.84
Travel	Gasoline for travel to site	\$309.80
Supplies	300-gallon tank & accompanying trailer	\$1,100
	Decatur handheld surface velocity radar	\$2,025
Supplies	Miscellaneous supplies for site operations	\$548.31
Total Awarded		\$5593.95
Total Remaining		\$0.00

1. Introduction

Five flood events were recorded at the Arroyo de los Piños sediment research station over the course of the 2018 monsoon season (Table 1). Water depth, velocity, suspended sediment, and bedload were collected manually during four of the events. Water depth, bedload, suspended sediment, turbidity, seismic, and acoustic data were collected automatically during all five (Table 2).

A photolog of all events can be found here: <https://drive.google.com/drive/folders/1z0j-esFqXPSs2HWDGLt3vZDoalPd9abb>

2. Results

Individual Event Summaries

Rainfall totals for the 2018 monsoon season are about 90% of the historical average. A total of 120 mm of rainfall was recorded at the upstream location while just 90 mm of rain was recorded at the site gauge near the basin outlet (Figure 1). However, the site gauge does not include data from the largest event (July 26th) because of an equipment malfunction during the event, accounting for much of the difference.

July 16th flood:

A moderate sized flood arrived as a single bore from runoff generated upstream. No rainfall was measured at the monitoring station while 16.8 mm of rainfall was recorded over one hour at the upstream location. Flow was recorded at the monitoring station for 3 hours (15:30 – 18:30). Seven suspended sediment and six bedload samples were collected manually. The automated ISCO samplers collected 22 and 5 samples from the upper (43 cm above the bed) and lower (6 cm above the bed) deployments, respectively. The storm cell moved quickly from south to north across the upper part of the basin (Figure 2)

July 26th flood:

The largest flood to date. Researchers arrived on site after flooding began; the road was not passable and the flood quickly became too dangerous to wade into. The monitoring station rainfall recorder malfunctioned in the first 30 minutes of the event, but 30 mm of rainfall was recorded at the upstream location. Flow was recorded at the monitoring station for 5.5 hours (22:00 – 03:30). Two manual suspended sediment samples were collected from the edge of the flood at the road crossing. The automated pump samplers malfunctioned during this event so no suspended sediment samples were collected. With such a large event, significant channel erosion and deposition occurred throughout the basin (see photolog). Bed incision from just downstream of the monitoring station to the Rio Grande confluence exceeded 0.5 m and nearly undermined the controlled cross section. The storm moved across the basin from north to south, with the highest intensity rainfall focused in the upstream part of the basin (Figure 3).

August 9th flood:

A relatively small flood was generated by runoff in the lower half of the watershed. (Figure 4). Flow was recorded at the monitoring station for 1.75 hours (22:45 – 00:30). Five suspended sediment and four bedload samples were collected manually. Twelve automated samples of suspended sediment were collected from the lower pump sampler inlet tube. Peak stage was below the upper sampler inlet tube.

August 24th flood:

A moderate sized flood was generated by runoff in the upper half of the watershed (Figure 5). Flow was recorded at the monitoring station for 2.75 hours (19:15 – 22:00). An extremely fast rising limb filled the slot samplers quickly. Seventeen automated samples of suspended sediment were collected.

September 1st flood:

Two separate storm cells passed across the basin within 3 hours (Figure 6). These storms produced low intensity rainfall, but wet antecedent conditions promoted the initiation of two small floods that reached the basin outlet. The first flood arrived at 09:30 while the second flood arrived at 12:30. Five automated and five manual samples of suspended sediment were collected.

Table 1: Basic Flood Characteristics.

Flood	Duration (hours)	Maximum Water Depth (cm)	Reach-average max bedload flux* (kg/sm)	Max suspended sediment concentration (mg/L)
July 16 th	3.00	60.0	6.0	104,000
July 26 th	5.50	161.0	12.0	No samples
Aug 9 th	1.75	16.5	4.0	29,600
Aug 24 th	2.75	32.0	12.0	90,100
Sept. 1 st	5.50 (two storms)	15.0	1.0	34,500 ⁺

* Reach-averaged bedload flux is measured directly using Reid-type slot samplers.

+ manual, vertically integrated sample

Table 2: Data collected during each event.

Flood date	Water depth	Bedload flux	Mic. Pulses	Seismic	Hydrophone	Turbidity	Suspnd. Sed.	Velocity
July 16 th	X, M	X, M	X	X		X	X, M	M
July 26 th	X	X	X	X	X*	X		
Aug. 9 th	X, M	X, M	X	X	X*		X, M	M
Aug. 24 th	X, M	X, M	X	X	X	X	X, M	M
Sept. 1 st	X, M	X, M	X	X	X		X, M	M

* only one of two hydrophone pairs recorded

X = collected automatically

M = collected manually

Water depth was fairly consistent across the channel during all floods (Figures 7 – 11). At lower flows, water was deeper on the left side of the channel (Figures 9 and 11). This is because the thalweg of the channel migrated to the left side after the July 26th event. Discharge estimates are not included in this report; more cross-channel velocity and depth measurements are necessary before developing a robust Piños rating curve.

Direct measurements of bedload flux were collected using Reid-type slot samplers. Two methods were tested to calibrate the slot samplers. For the right and center samplers, mass was loaded systematically into each sampler. The response of the pillow transducer was recorded and a regression line was fit. For the left sampler, all mass was added and then unloaded systematically. Both methods showed good calibration between added mass and transducer response (Figure 12).

Bedload flux was calculated using the response from the pillow transducer and the calibration curve. Measurements were taken every minute and a 3-minute averaging window was applied to smooth the data. Bedload flux varied widely between events. In moderate flows, the Reid slot samplers filled extremely fast. During the large July 26th event, two of the samplers were filled in less than 20 minutes (Figure 13). In general, bedload flux increased with water depth (Figure 14), although there is a large variation due to the pulsed nature of bedload flux. The highest reached-averaged fluxes are reported in Table 1 but the highest observed bedload flux at any single sampler was measured during the July 26th event (16.5 kg/sm).

Each Reid slot sampler is co-located with a surrogate bedload-measuring instrument. The right and left samplers have pipe microphones while the center sampler has a plate microphone installed directly upstream of the sampler. These surrogate methods measure the acoustic signal of bedload impacting the plate or pipe. If the response exceeds some threshold, a pulse is counted. Ten amplifications of the acoustic response are recorded by each microphone (Figure 15). The highest amplifications (P1024, P512, and P256) have the lowest threshold to record a pulse. As such, they are often saturated during events. If these three are removed, the remaining amplifications show sequentially higher numbers of recorded pulses (Figure 16). These pulses are accumulated over one minute and the same 3-minute averaging window is applied for comparison to calculated bedload flux values. Other surrogate instruments to measure bedload include seismometers and hydrophones (Table 2). These data are collected in collaboration with other researchers and are evaluated by those collaborators.

Samples of suspended sediment were collected using ISCO 3700 pump samplers. These samplers automatically collected samples throughout the flood from two vertical locations at the stilling well located on river right. These samples are augmented by manual samples collected across the channel. During the 2018 monsoon season, 81 discrete samples of suspended sediment were collected. These samples were dried and weighed to determine the suspended sediment concentration (Figure 17). Samples collected during the falling limb of the hydrograph show a general linear trend increasing with water depth. Samples collected during the rising limb and at maximum water depth depart from this trend and have a higher concentration for a given water depth.

3. Figures:

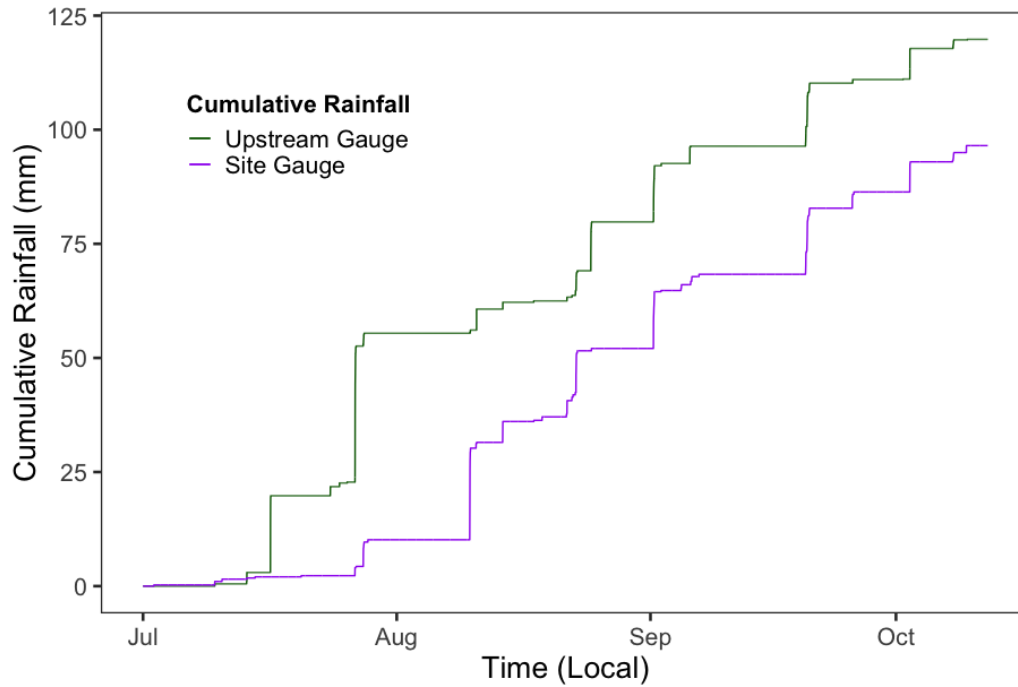


Figure 1: Cumulative Rainfall in mm for the 2018 monsoon season. Data are missing from the site gauge for the July 26th event because of an equipment malfunction.

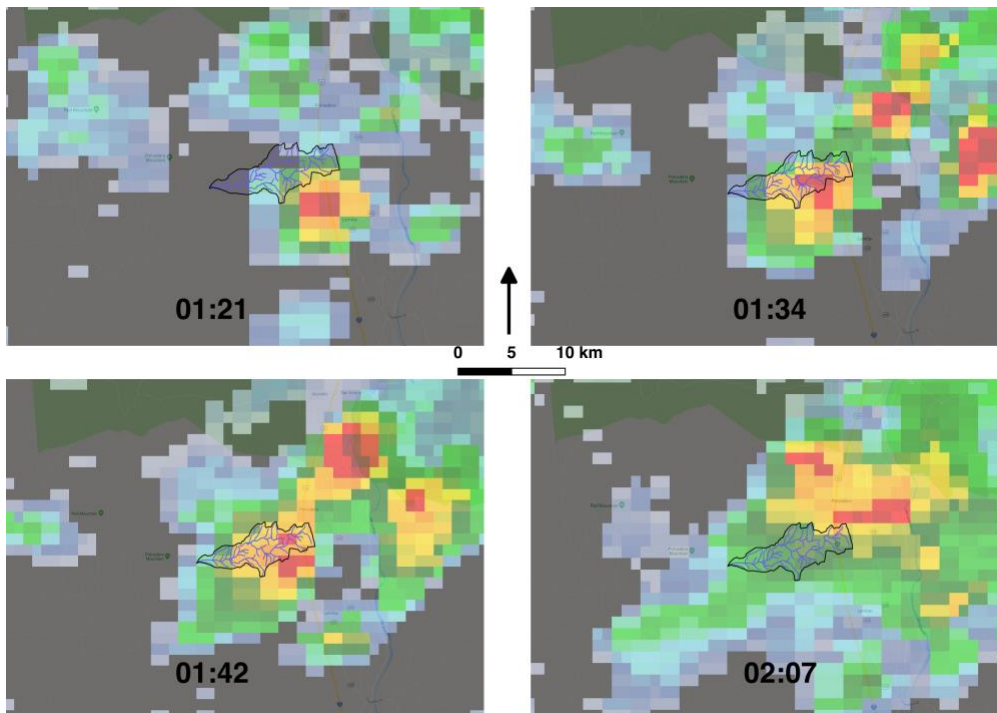


Figure 2: July 16th, 2018 storm movement captured by NEXRAD. Warmer colors indicate higher rainfall intensities. A moderately sized cell caused 17 mm of rainfall at the upstream location.

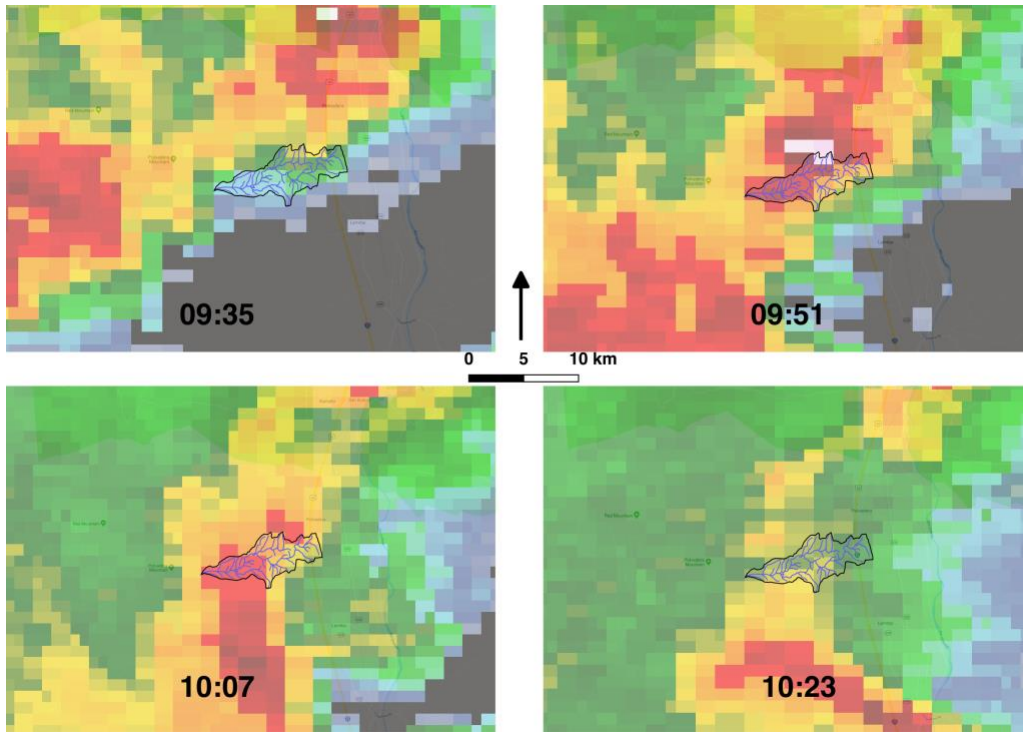


Figure 3: July 26th, 2018 storm movement captured by NEXRAD. Warmer colors indicate higher rainfall intensities. A large cell caused high intensity rainfall throughout the basin. 30 mm of rain were recorded at the upstream location.

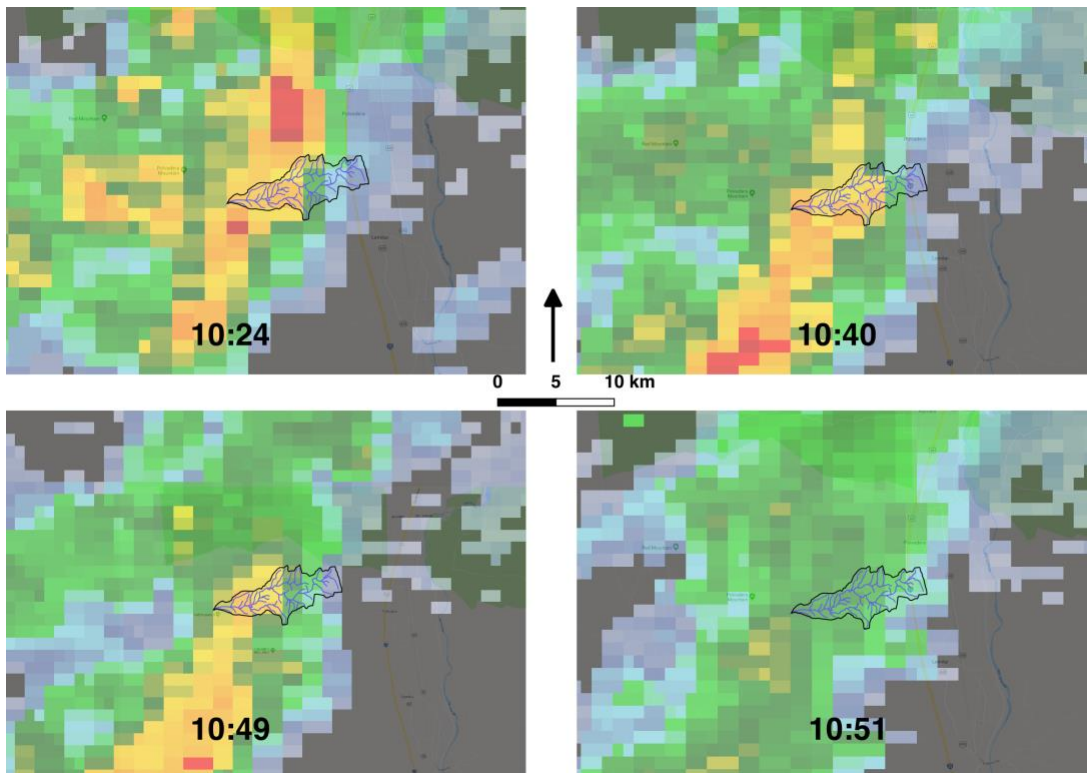


Figure 4: August 9th, 2018 storm movement captured by NEXRAD. Warmer colors indicate higher rainfall intensities. Rainfall was focused on the lower half of the watershed.

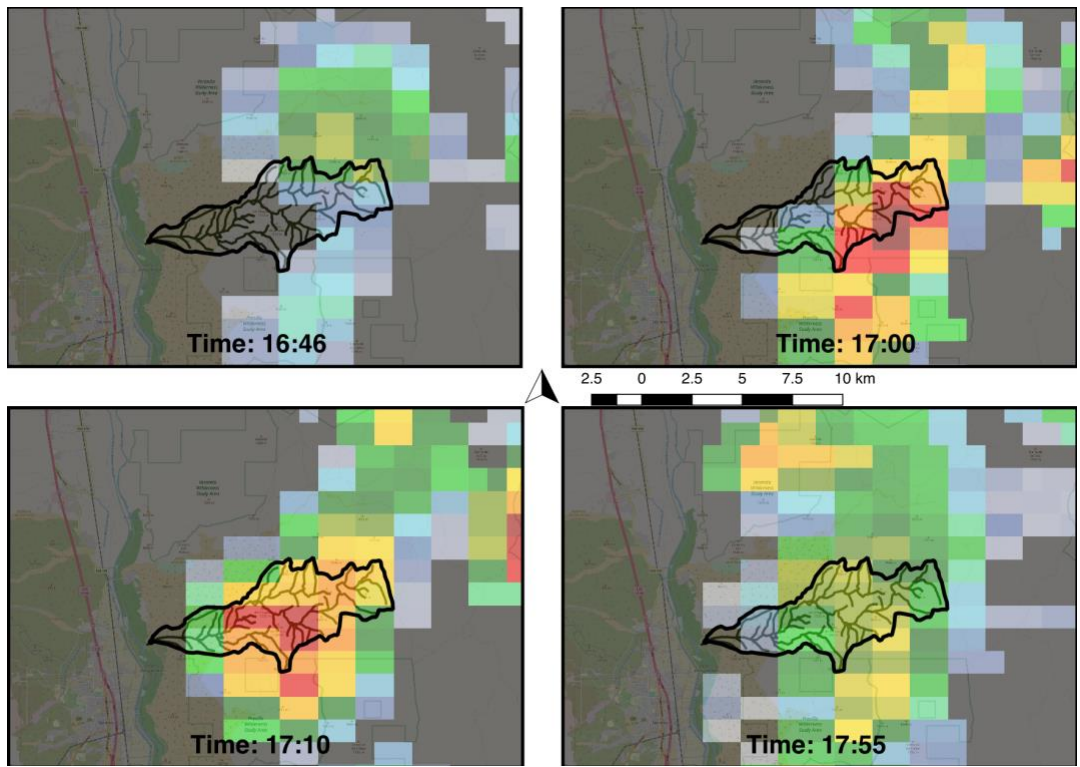


Figure 5: August 24th, 2018 storm movement captured by NEXRAD. Warmer colors indicate higher rainfall intensities. Rainfall was focused on the lower half of the watershed.

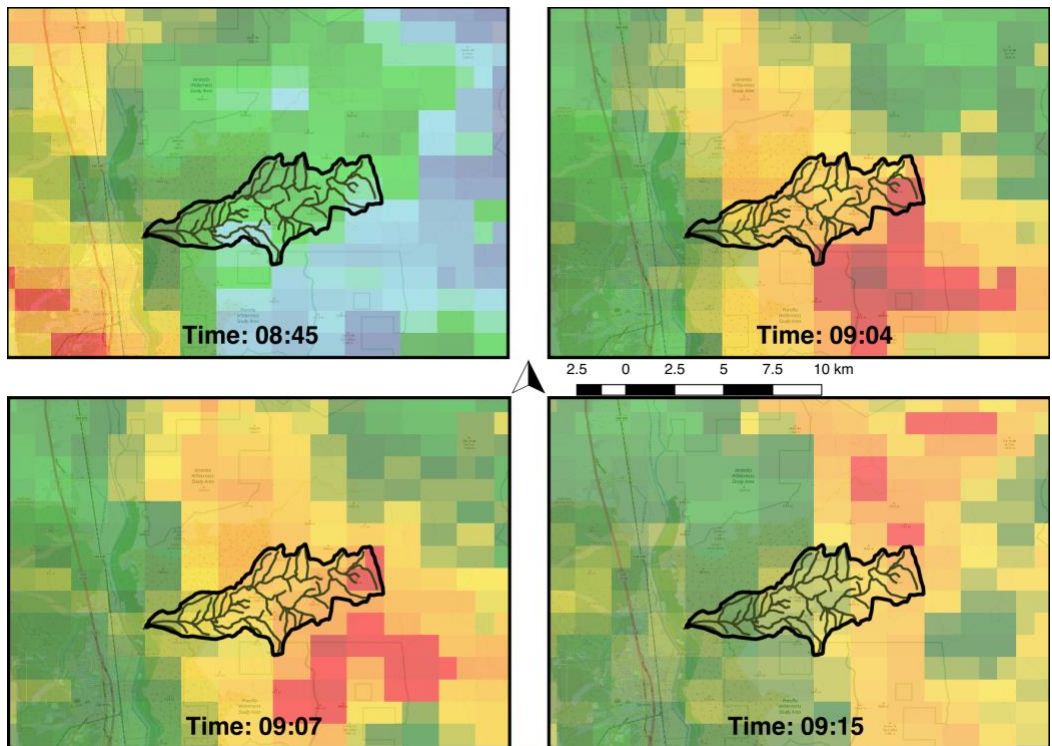


Figure 6: September 1st, 2018 storm movement captured by NEXRAD. Warmer colors indicate higher rainfall intensities. Rainfall was focused on the lower half of the watershed.

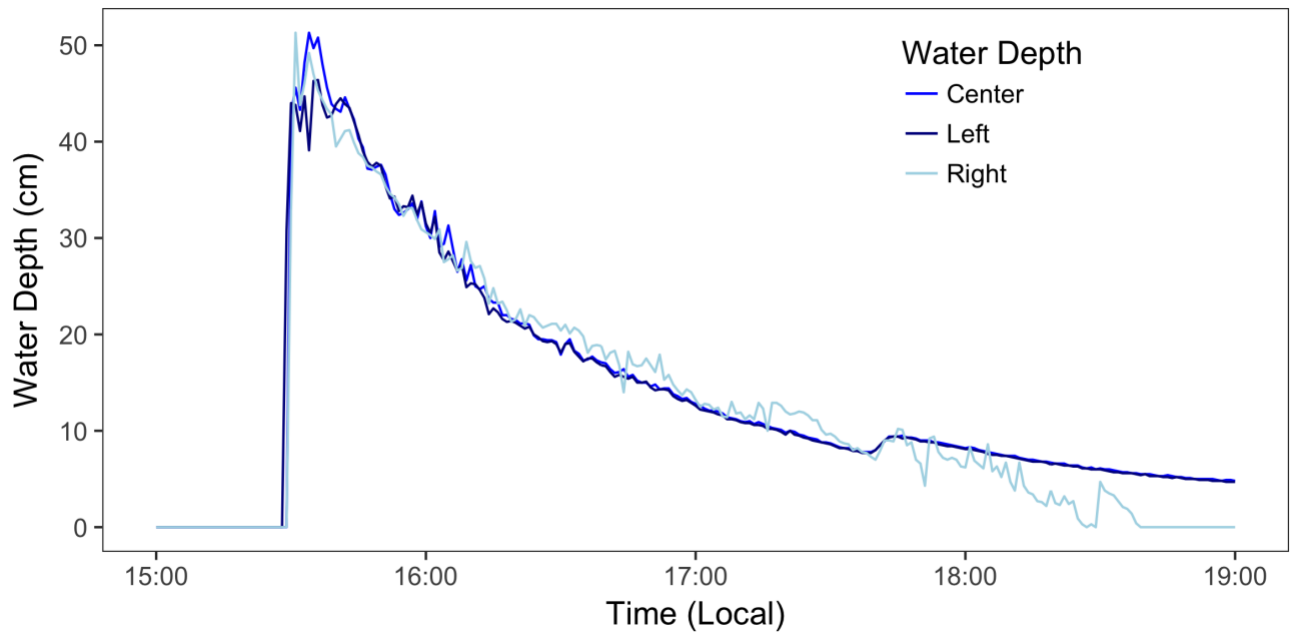


Figure 7: Water depth measured during the July 16th flood event as recorded by the stage pressure transducers located in each of the Reid slot samplers.

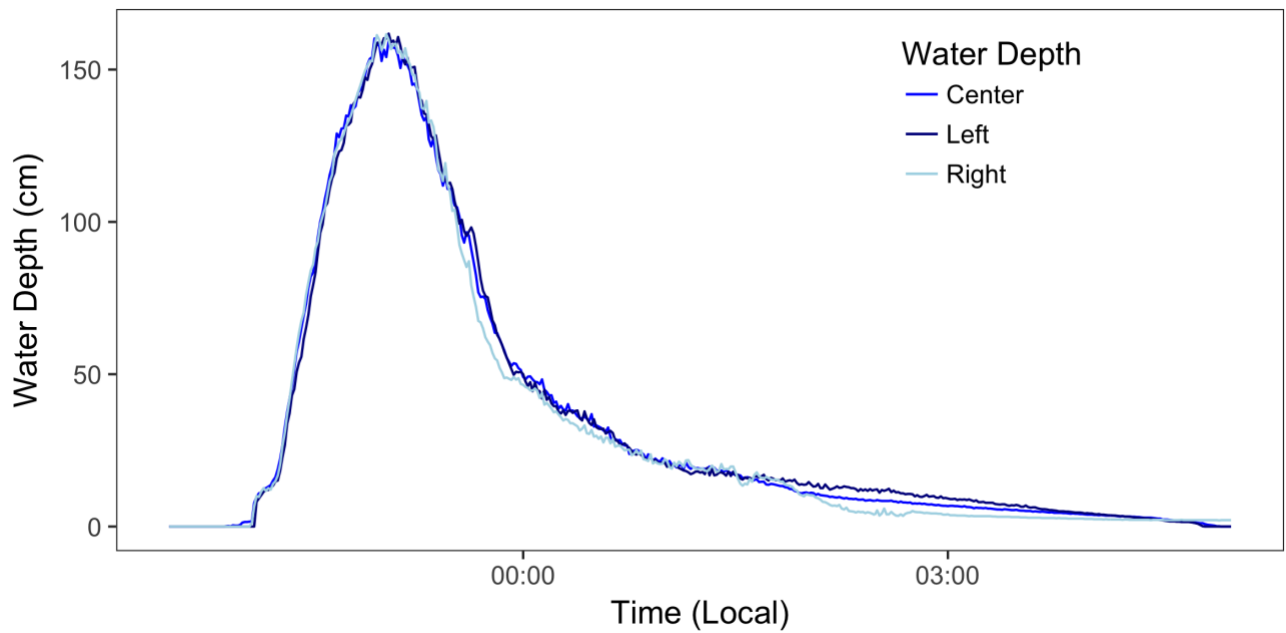


Figure 8: Water depth measured during the July 26th flood event as recorded by the stage pressure transducers located in each of the Reid slot samplers.

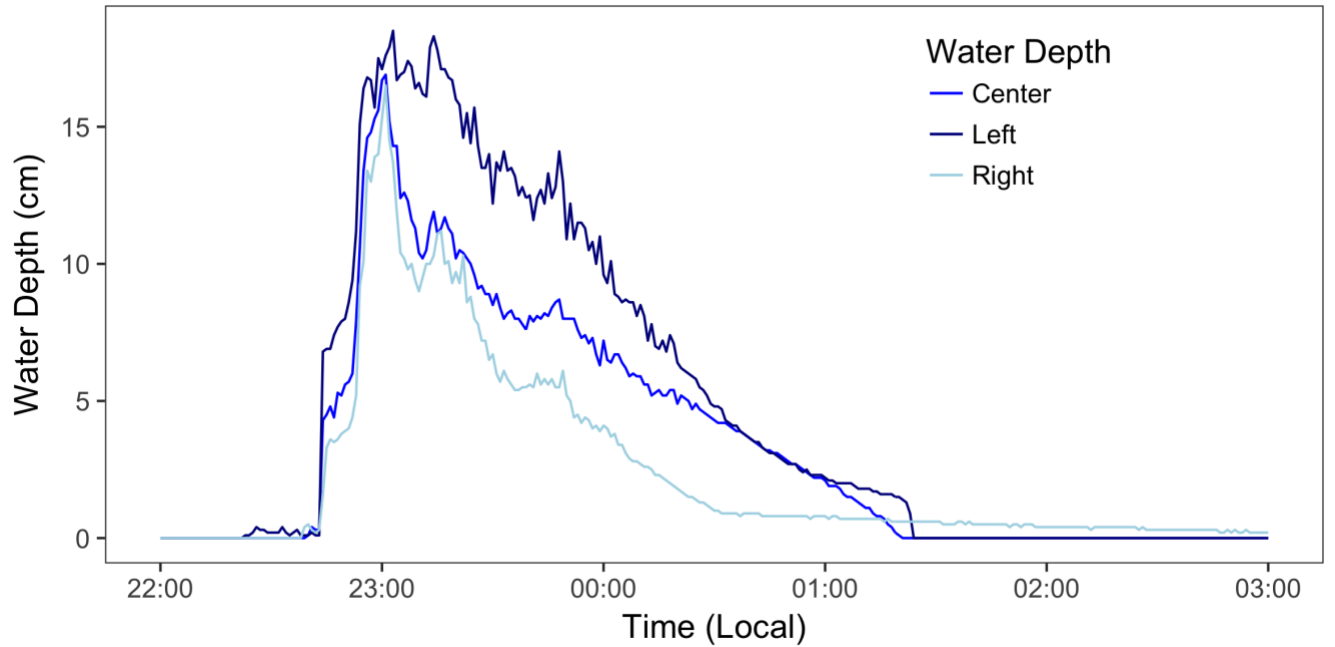


Figure 9: Water depth measured during the August 9th flood event as recorded by the stage pressure transducers located in each of the Reid slot samplers. Focused flow on the river left thalweg was observed during this event.

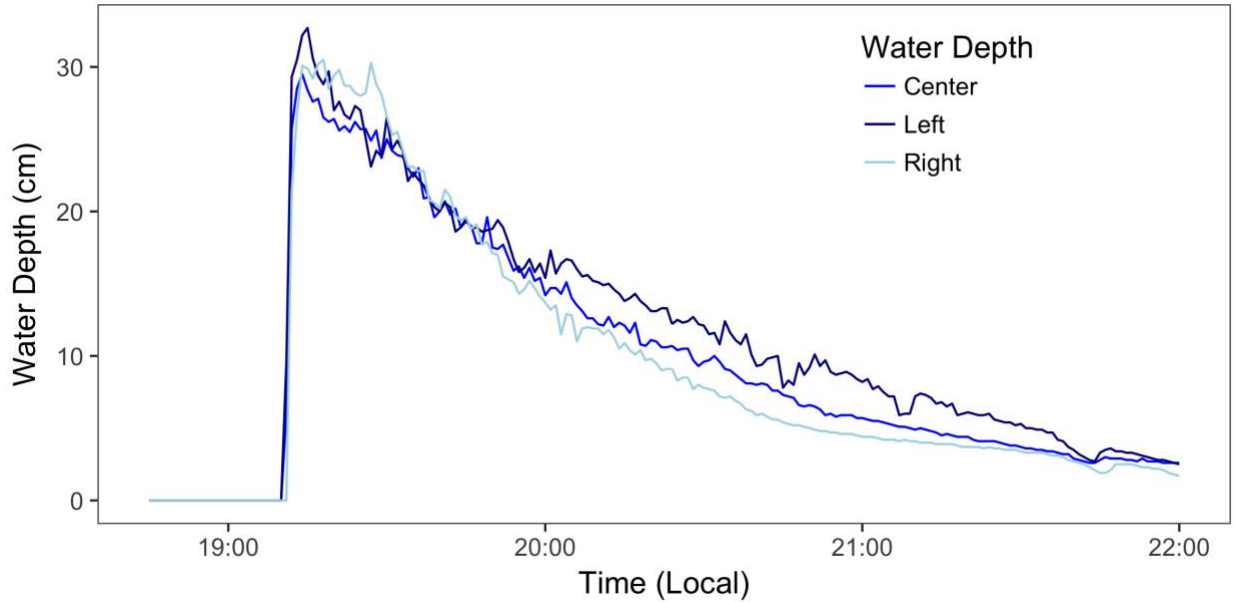


Figure 10: Water depth measured during the August 24th flood event as recorded by the stage pressure transducers located in each of the Reid slot samplers.

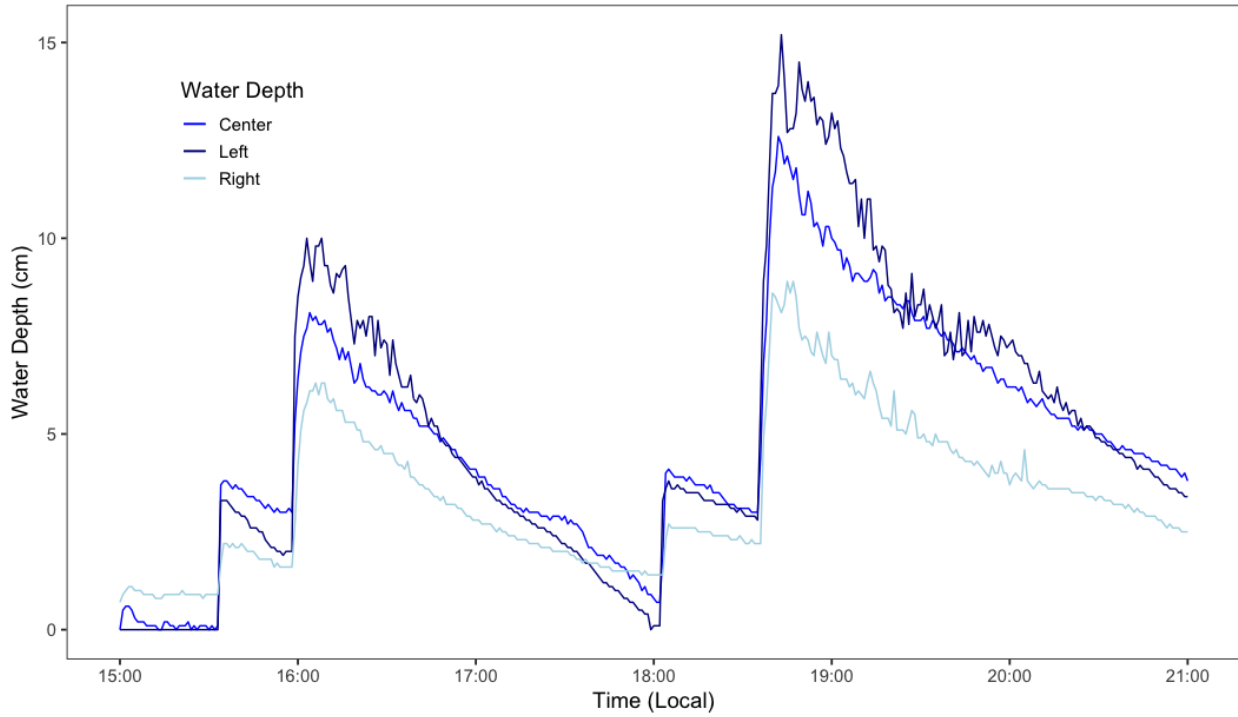


Figure 11: Water depth measured during the September 1st flood event as recorded by the stage pressure transducers located in each of the Reid slot samplers.

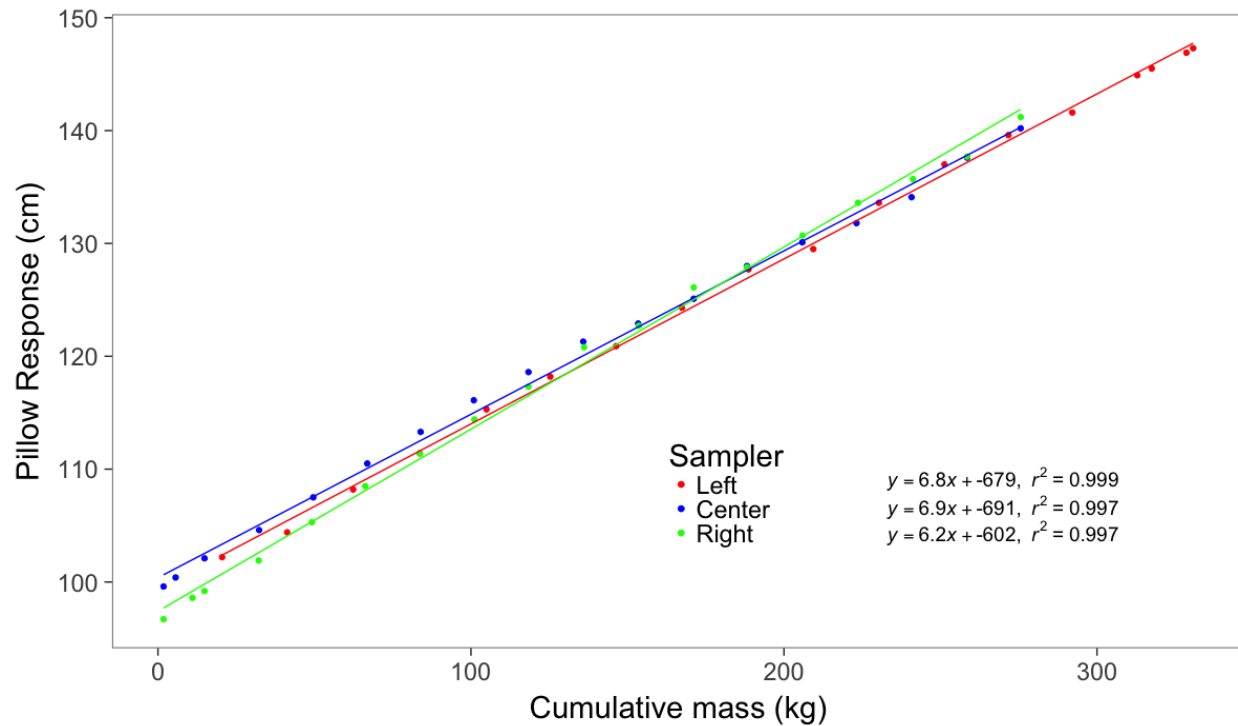


Figure 12: Pillow calibration for the 2018 field season. Known mass are incrementally added to each Reid slot sampler and the pillow response is observed. All three show strong correlations ($r^2 > 0.997$).

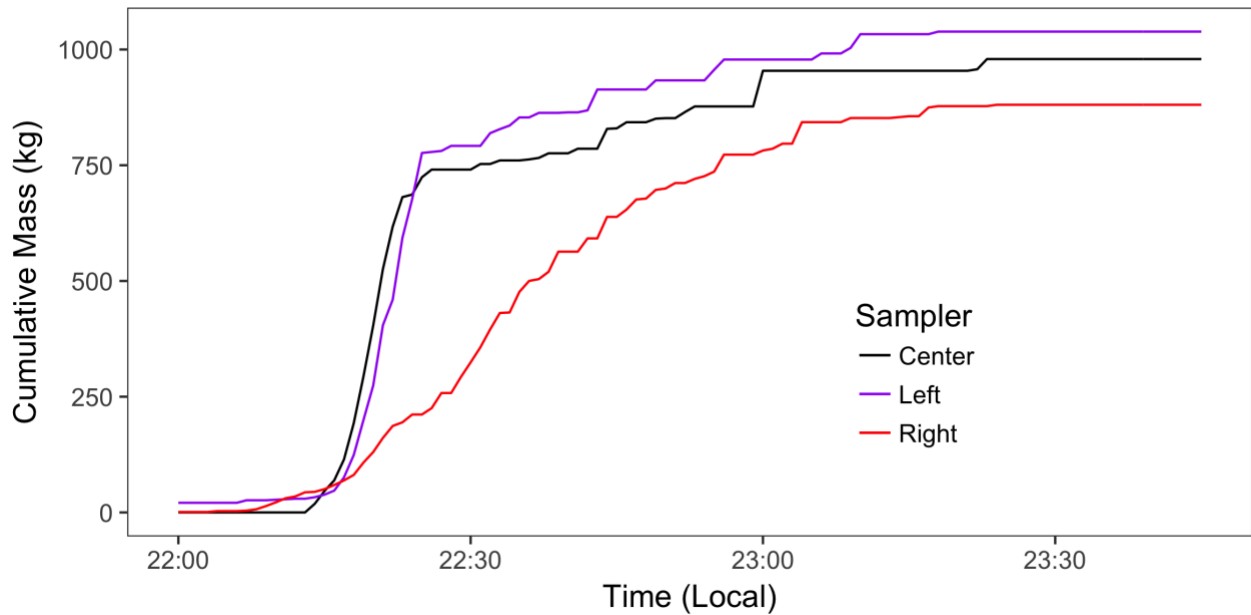


Figure 13: Sediment accumulating inside each Reid slot sampler during the July 26th flood event. The center and left samplers reached near capacity within 20 minutes of the first flood wave recorded at the site.

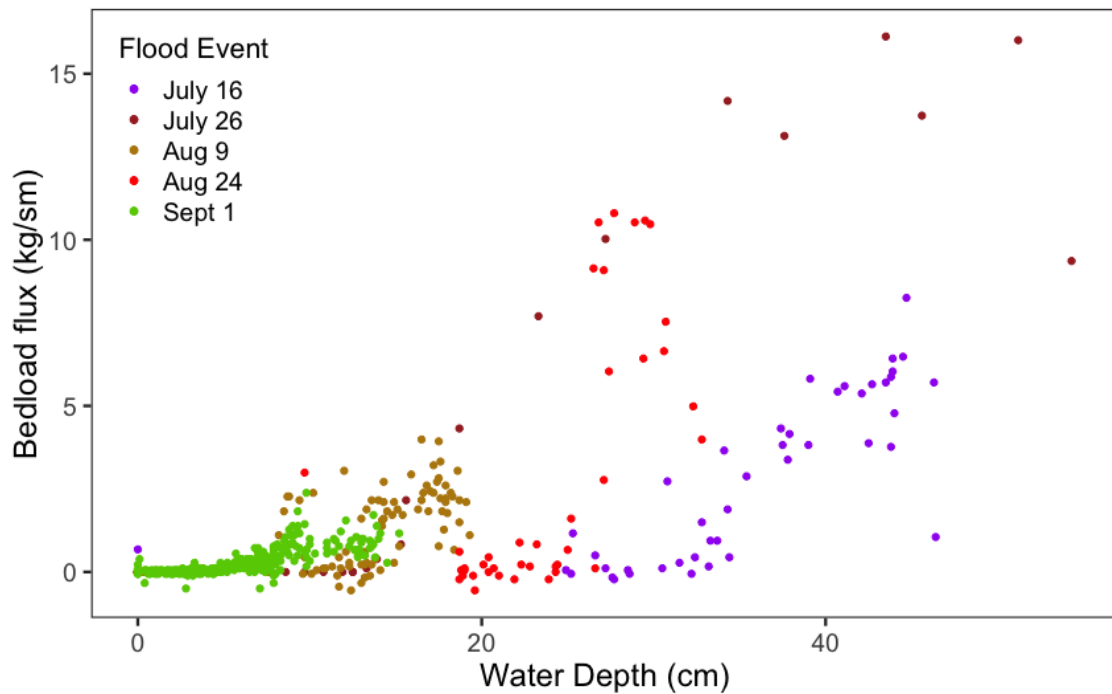


Figure 14: Calculated bedload flux from the left Reid slot sampler. Globally high rates of bedload flux were observed.

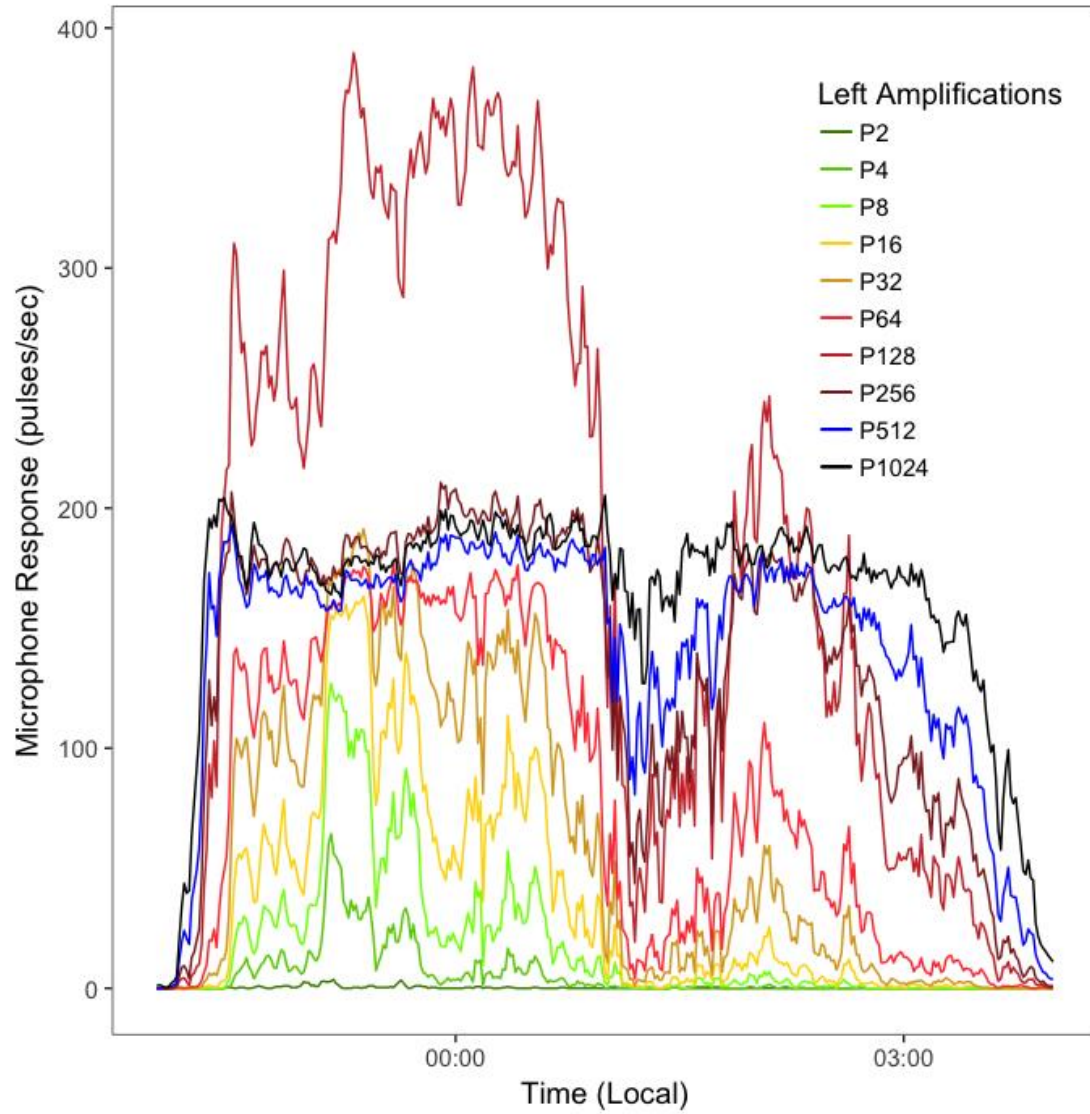


Figure 15: Acoustic response from the left pipe microphone during the July 26th event. Amplifications P1024, P512, and P256 are all saturated during the highest bedload flux rates.

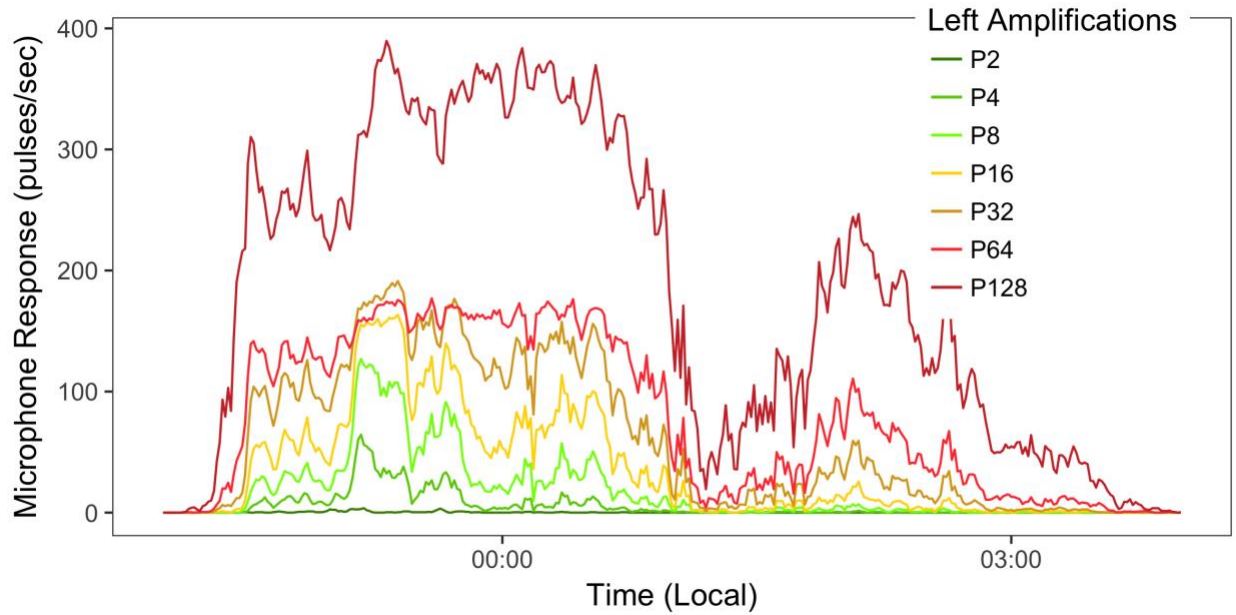


Figure 16: Acoustic response from the left pipe microphone during the July 26th event with the saturated amplifications removed. Each amplification records sequentially higher number of pulses.

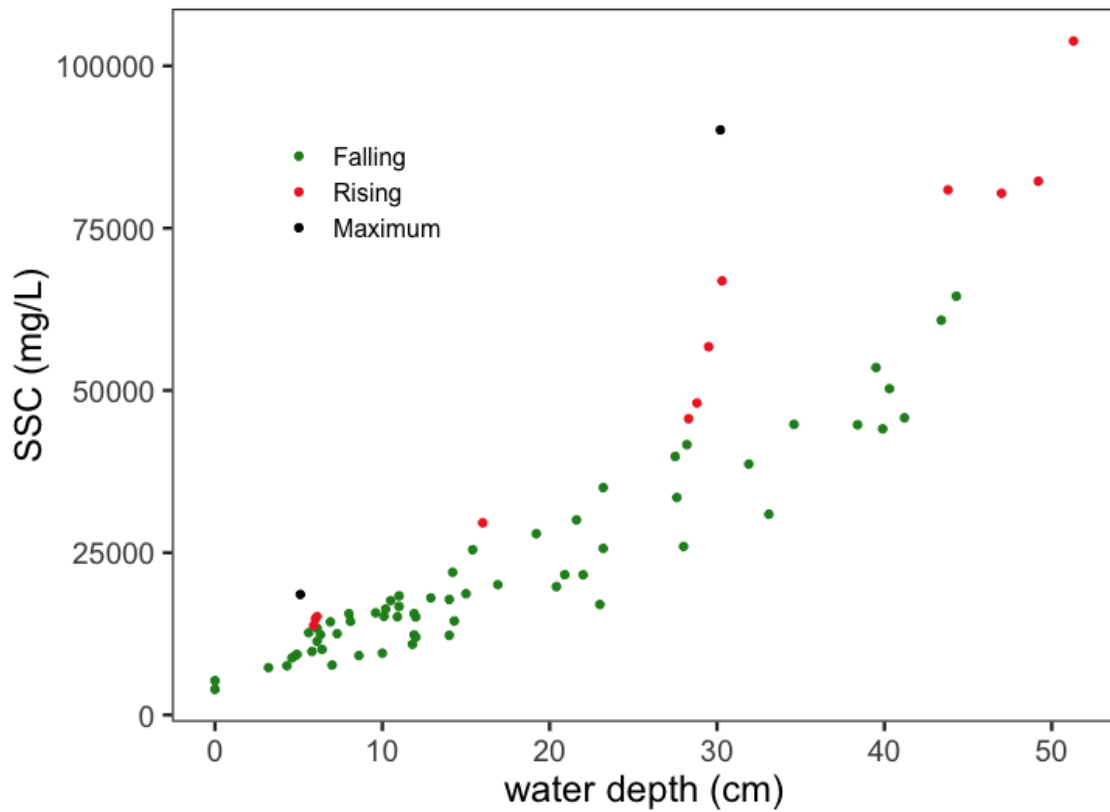


Figure 17: SSC as a function of water depth. Red and black samples were collected during the rising limb and maximum flow and show a higher SSC when compared to samples collected on the falling limb at the same depths.

4. Conclusions:

Data collected from the first fully-operational monsoon season highlights the strengths of the Piños sediment monitoring station. The amount of data collected is enormous; a full analysis of these data will require multiple years to compare the results between flows. To date, the top line results reveal a system that is highly efficient at mobilizing sediment. Surrogate methods for measuring these sediment fluxes are required as traditional methods (i.e. Reid slot samplers) fill quickly and are rendered inoperable in these environments. Future monsoon seasons will incorporate new instruments to measure velocity and other key hydrograph features that can be used to better describe the sediment transport within the Piños.

5. Acknowledgements:

Project funding comes from the U.S. Army Corps of Engineers, U.S. Bureau of reclamation, and from the New Mexico Water Resources Institute and NM State legislator grant #: NMWRRI-SG-2018. The authors would like to specifically thank students Madeline Richards and Jared Ciarico for the enormous help gathering and processing the data presented here.